TIME-FREQUENCY REPRESENTATIONS OF EARTHQUAKE MOTION RECORDS

Sorin Demetriu, Romică Trandafir

Abstract

Time-frequency representations are considered for energetic characterization of the nonstationary accelerograms recorded during strong Vrancea earthquakes. Performances of different time-frequency quadratic distributions are compared. The results can be used to evaluate the destructive potential of strong motion seismic records.

1 Introduction

The evolution of the amplitude/energy/power characteristics is an essential feature of nonstationary time series. The time variation of these characteristics with the frequency content is given by spectral representations in two-dimensional time-frequency domain (Cohen, 1995; Flandrin, 1999; Hlawatsch and Boudreaux-Bartels, 1992; Matz and Hlawatsch, 2003). In this paper, nonparametric time-frequency distributions are used to describe the energy of the components of ground acceleration recorded on three orthogonal directions during a strong earthquake.

2 Time-frequency representations

Multiple resolution representations describe the signature of nonstationary signal in the time-frequency or time-scale parameter domain, showing slow variations or sudden changes of the energy and amplitude characteristics. Time-frequency distributions represent some extensions of stationary spectral functions in relationship with the time variable. The wavelet representation is a local description for several scales of resolution. Nonstationary spectral analysis includes efficient numerical procedures (FFT algorithms) for computing discrete transformations and components for graphical representations of images, surfaces and contours with the same level of intensity.

The following categories of nonparametric distributions can be considered (Cohen, 1995; Flandrin, 1999; Hlawatsch and Boudreaux-Bartels, 1992):

(1) linear distributions: Short-time Fourier transform (STFT), Gabor;

(2) Cohen class bilinear distributions: Spectrogram (SP), Wigner-Ville (WV), Pseudo-Wigner-Ville (PWV), Smoothed Pseudo Wigner-Ville (SPWV), Butterworth (BU), Born-Jordan (BJ), Morgenau-Hill (MH), Pseudo Morgenau-Hill (PMH), Reduced interference (RI) with different kernels (Bessel, Hanning), Choi-Williams (CW), Rihaczec, Page (PAG), Zhao-Atlass-Mark (ZAM);

(3) reassigned time-frequency distributions: Reassigned Spectrogram (R-SP), Reassigned Wigner–Ville (R-WV), R-PWV, R-SPWV, R-PPAG, R-PMH;

(4) affine class bilinear distributions: Bertrand, Wavelet (Scalogram).

The amplitude distribution is described by the short-time Fourier transform through the linear integral

$$STFT_x^{(h)}(t,f) = \int_{-\infty}^{\infty} x(\tau) \cdot h(\tau - t) \cdot \exp(-i \cdot 2\pi f \tau) d\tau. \qquad (2.1)$$

STFT is the local spectrum of signal $x(t)$ around time t, selected by localization window $h(t)$. For discrete signals, with bounded duration and frequency band, considering that $t_n = n \cdot \Delta t$, $f_k = k \cdot \Delta f$, $\tau_m = m \cdot \Delta t$, where Δt and Δf are sampling time and frequency intervals, STFT can be obtained through FFT algorithms.

Spectrogram (SP) is the short-time quadratic integral measure of the energy distribution

$$SP_x^{(h)}(t,f) = \left| STFT_x^{(h)}(t,f) \right|^2 = \left| \int_{-\infty}^{\infty} x(\tau) \cdot h(\tau - t) \cdot e^{-i \cdot 2\pi f \tau} d\tau \right|^2. \quad (2.2)$$

Two-dimensional time-frequency representations of the energy of one-dimensional signal $x(t)$ are quadratic transformations $T_x(t,f)$ which combine both concepts of instantaneous power and energy spectral density. These one-dimensional marginal functions are given by:

– energy spectral density: $|X(f)|^2 = \int_{-\infty}^{\infty} T_x(t,f) dt,$

– instantaneous power: $|x(t)|^2 = \int_{-\infty}^{\infty} T_x(t,f) df,$

and are used to obtain the total energy

$$E_x = \int_{-\infty}^{\infty} \int_{-\infty}^{\infty} T_x(t,f) dt df = \int_{-\infty}^{\infty} |x(t)|^2 \, dt = \int_{-\infty}^{\infty} |X(f)|^2 \, df$$

In the two-dimensional time-frequency domain the energy distribution is described by the shift-invariant quadratic transformations (Cohen class):

$$T_x(t,f) = \int_{-\infty}^{\infty} \int_{-\infty}^{\infty} \Psi_x(\tau,\nu) A_x(\tau,\nu) \cdot \exp(i \cdot 2\pi(t\nu - f\tau)) d\tau d\nu, \qquad (2.3)$$

where

$$A_x(\tau,\nu) = \int_{-\infty}^{\infty} x\left(t + \frac{\tau}{2}\right) \cdot x^*\left(t - \frac{\tau}{2}\right) \cdot \exp(-i \cdot 2\pi\nu t) dt =$$

$$= \int_{-\infty}^{\infty} X\left(f + \frac{\nu}{2}\right) \cdot X^*\left(f - \frac{\nu}{2}\right) \cdot \exp(i \cdot 2\pi f\tau) df, \qquad (2.4)$$

$$\Psi_x(\tau,\nu) = \int_{-\infty}^{\infty} \int_{-\infty}^{\infty} \psi_x(\tau,\nu) \cdot \exp(i \cdot 2\pi(t\nu - f\tau)) dt df, \qquad (2.5)$$

and $\psi_x(t,f)$ and $\Psi_x(\tau,\nu)$ are the signal-independent transformation kernels in the time-frequency (t,f) plane and in the ambiguity time lag-frequency lag (τ,ν) plane, respectively. The ambiguity function (AF) $A_x(\tau,\nu)$ and the Wigner-Ville distribution (WV) form a two-dimensional transforms pair:

$$WV_x(t,f) = \int_{-\infty}^{\infty} \int_{-\infty}^{\infty} A_x(\tau,\nu) \exp[i \cdot 2\pi(t\nu - f\tau)] d\tau d\nu. \qquad (2.6)$$

The forms of the transformation kernel $\Psi_x(\tau,\nu)$ for some distributions used in applications (Hlawatsch and Boudreaux-Bartels, 1992; Hlawatsch et al., 1995) are shown in Table 1.

Due to the bilinearity of the quadratic transformations, the cross-terms yield false ordinates that can mask the true spectral components of the signal. A two-dimensional smoothing low-pass filtering can be used to reduce these interference effects, but this can lead to a lower resolution and to the degradation of some of the distribution properties. In establishing the location in time-frequency domain, Cohen class transformations are sensitive to the properties and type of distribution kernel and two-dimensional smoothing window. Reassignment methods lead to some distribution versions which allow an improvement in the representation and localization details in time-frequency domain.

Table 1: Different forms of the transformation kernel $\Psi_x(\tau, \nu)$.

Distribution	$\Psi_x(\tau, \nu)$
Wigner-Wille (WVD)	1
Pseudo WignerWille (PWV)	$\eta(\frac{\tau}{2}) \cdot \eta^*(-\frac{\tau}{2})$, η – lowpass window function
Smoothed PWV (SPWV)	$\eta(\frac{\tau}{2}) \cdot \eta^*(-\frac{\tau}{2}) \cdot G(\nu)$, $G(\nu)$ – spectral window
Choi-Williams (CWD)	$\exp\left(-\frac{(2\pi\tau\nu)^2}{\sigma}\right)$, $\sigma \in (0.1, 1)$
Spectrogram (SP)	$A_h(-\tau, -\nu)$, AF of localization window $h(t)$
Generalized Exponential (GE)	$\exp\left[-\left(\frac{\tau}{\tau_0}\right)^{2M}\left(\frac{\nu}{\nu_0}\right)^{2N}\right]$
Butterworth (BU)	$\frac{1}{1+\left(\frac{\tau}{\tau_0}\right)^{2M}\left(\frac{\nu}{\nu_0}\right)^{2N}}$
Gaussian	$\exp\left\{-\pi\left[\left(\frac{\tau}{\tau_0}\right)^2 + \left(\frac{\nu}{\nu_0}\right)^2 + 2r\left(\frac{\tau\nu}{\tau_0\nu_0}\right)\right]\right\}$
Cone-Kernel	$g(\tau) \cdot |\tau| \cdot \frac{\sin(\pi\tau\nu)}{\pi\tau\nu}$

3   Time-frequency representations of seismic accelerograms

The accelerograms analyzed below represent benchmark data for engineering applications. Table 2 includes: characteristics of the 1977, 1986 and 1990 Vrancea earthquakes; the parameters adopted for processing the data (sampling time interval, filtering frequency band-pass); peak values of ground acceleration (PGA), ground velocity (PGV) and ground displacement (PGD) of the translational components recorded on three orthogonal directions; and total duration of these records and total cumulative energy (ECT) of the accelerations. The series were obtained by INCERC through uniform time discretization of instrumental data records following a standard procedure that removes tendencies and instrument effects, and filters discretization and measurement noise. Corrected accelerograms are representative for their frequency band-pass filtering. The database also include the velocity and displacement components obtained through numerical integration of the digitized accelerations.

Some of the following results were obtained using the time-frequency tool-

Table 2: Characteristics of earthquake records at INCERC Bucharest.

Vrancea earthquake	Distance from source	Filtering band (Hz)	Sampling interval (s)	Comp	Duration of record (s)	Peak values			ECT $(*10^3)$ cm^2/s^3
						PGA cm/s^2	PGV cm/s	PGD cm	
4.03.1977		0.15(0.35)		NS	65.36	207.6	67.93	16.18	55.5
$M_{G-R}=7.2$	148 km	-	0.005	EW	66.39	181.3	29.92	9.01	33.8
$h_F=133$ km		25(28)		VERT	64.93	122	10.12	2.33	13.1
30.08.1986		0.15(0.35)		NS	47.96	96.96	15.51	3.75	9.07
$M_{G-R}=7$	181 km	-	0.005	EW	47.96	109.1	11.31	2.56	8.25
$h_F=133$ km		25(28)		VERT	47.96	20.66	2.71	0.58	0.92
30.05.1990		0.15(0.35)		NS	49.34	66.21	6.35	1.06	4.81
$M_{G-R}=7$	187 km	-	0.005	EW	52.48	98.91	16.97	2.91	8.45
$h_F=91$ km		25(28)		VERT	52.85	27.97	2.75	0.56	0.86

box developed in MATLAB (Auger et al., 1996).

The time-frequency energy distributions (spectrograms) of the accelerations recorded at INCERC Bucharest site during the 1977, 1986 and 1990 earthquakes on three orthogonal directions (NS, EW, VERTICAL) are represented in Figures 1, 2 and 3.

Figures 4 and 5 display different quadratic distributions obtained for a representative segment of 40 seconds from the NS-accelerogram recorded during the 1977 Vrancea earthquake. The results show the performance of different representations in locating the energy distribution in time-frequency domain. The SP and SPWV representations allow localization with enough clarity, their precision being determined by the time and frequency resolution. Using the RSP and RSPWV reassigned distributions, the quality of representation and location details is significantly improved. Also, notice the cross-term interference effects due to the bilinearity of the Wigner-Ville and Choi-Williams transformations.

The marginal densities and cumulative distributions, in time and frequency respectively, of the energy of acceleration components recorded during the 1977 Vrancea earthquake are shown in Figure 6.

4   Conclusions

Energy distribution of accelerograms in time-frequency domain illustrate the effects of seismic source, wave propagation and local soil conditions, allowing the assessment of the destructive potential of motions recorded in free field sites. Time-frequency analysis can be applied to instrumented buildings, where energy distributions of the seismic response recorded during earthquakes show variations of modal and response parameters. These distributions can be used for damage identification, performance monitoring and diagnosis of structural systems (Demetriu, 2001). Time-frequency analysis can also be extended to

the nonstationary time series obtained by recording the velocity/pressure of turbulent winds or wave height during storms.

REFERENCES

1. Auger, F., Flandrin, P., Goncalves, P. and Lemoine, O. *Time-Frequency Toolbox*, CNRS France - Rice University, 1996.

2. Cohen, L. *Time Frequency Analysis*, Prentice-Hall, New Jersey, 1995.

3. Demetriu, S. *Structural Identification of Existing Buildings from Earth-quake Motion Records*, in D. Lungu & T. Saito, eds., Earthquake Hazard and Countermeasures for Existing Fragile Buildings, pp. 223-236, 2001.

4. Flandrin, P. *Time-Frequency/Time-Scale Analysis*, Academic Press, 1999.

5. Hlawatsch, F., and Boudreaux-Bartels, G.F. *Linear and Quadratic Time-Frequency Signal Representations*, IEEE SP Magazine, pp. 21-67, April, 1992.

6. Hlawatsch, F., Manickam, T. G., Urbanke, R. L, and Jones, W. *Smoothed pseudo-Wigner distribution, Choi-Williams distribution, and cone-kernel representation: Ambiguity-domain analysis and experimental comparison*, Signal Processing, vol. 43 (2), pp. 149-168, 1995.

7. Matz, G., and Hlawatsch, F. *Wigner distributions (nearly) everywhere: time-frequency analysis of signals, systems, random processes, signal spaces, and frames*, Signal Processing, Vol. 83(7), 2003.

Technical University of Civil Engineering
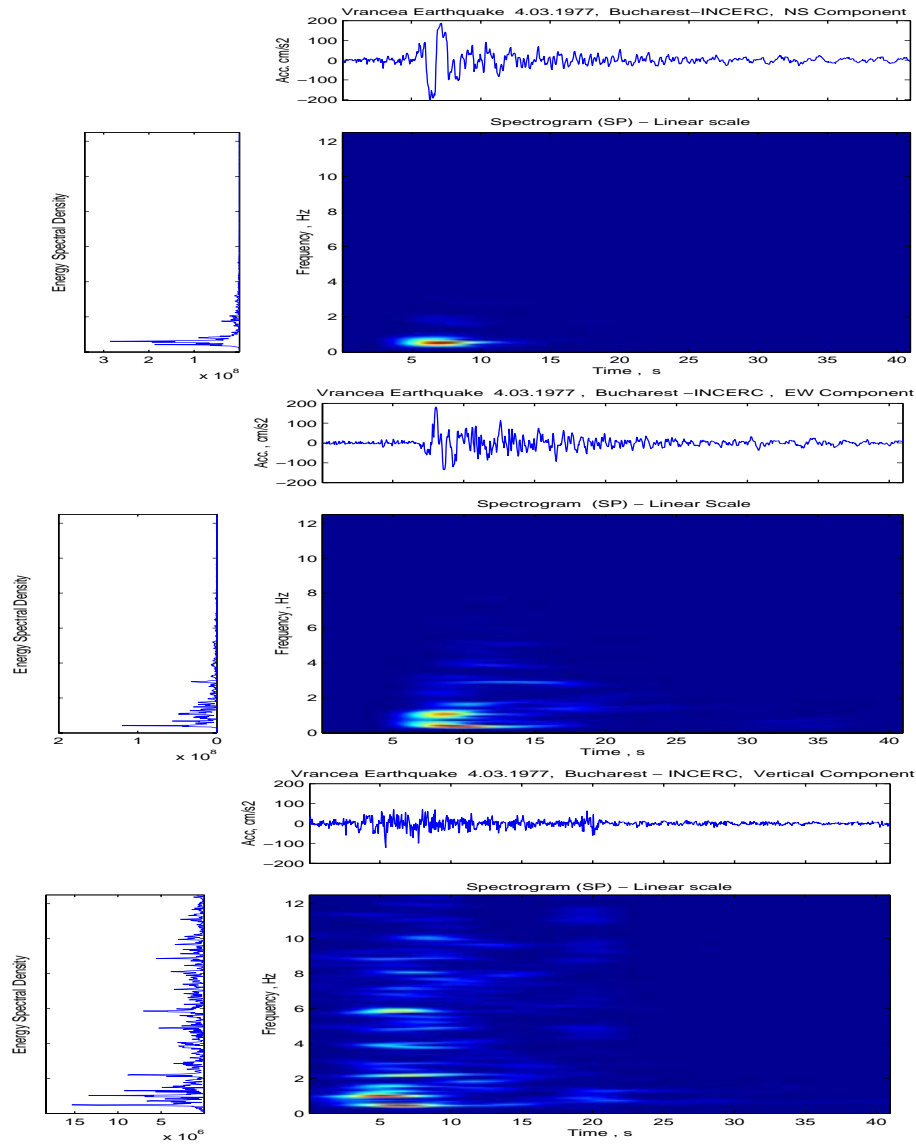124 Bd. Lacul Tei, sect. 2, Bucharest 020396

Fig. 1. Time-frequency representation (Spectrogram) of accelerograms recorded during the
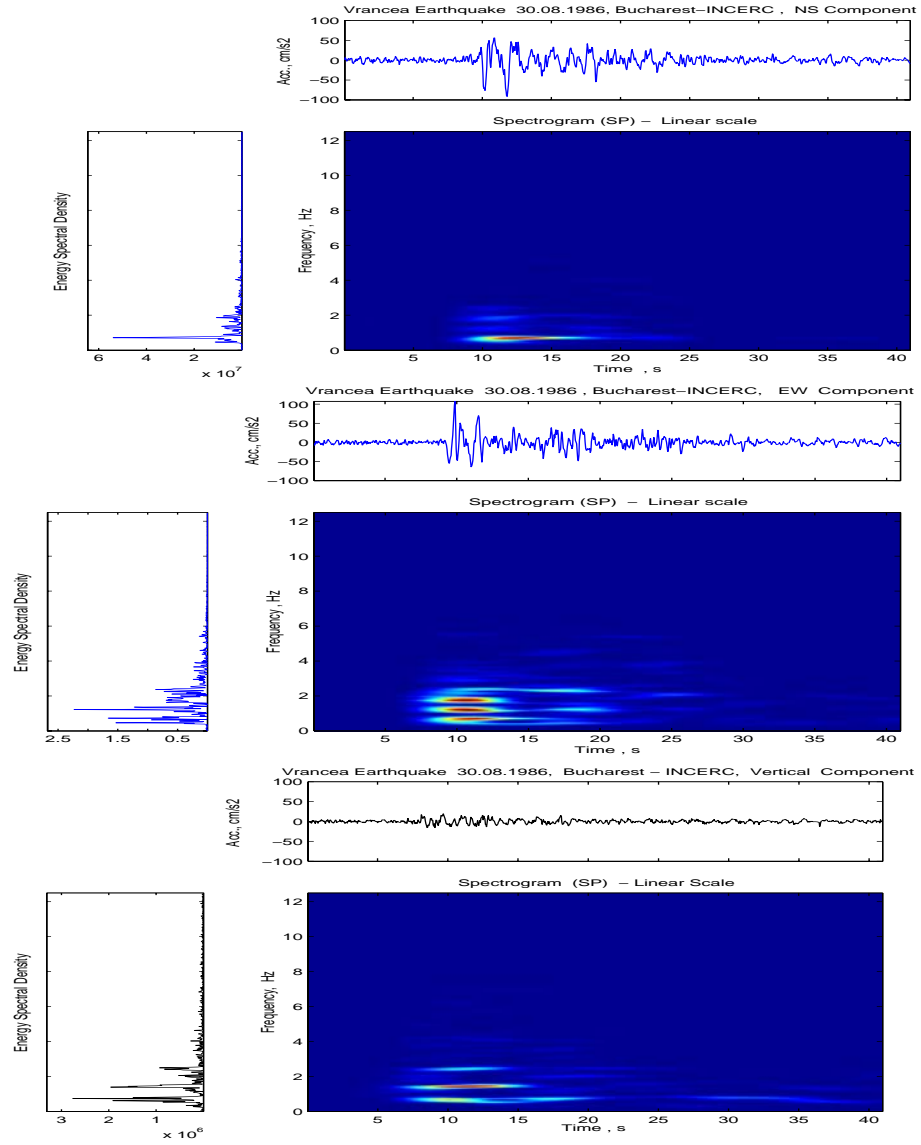1977 Vrancea earthquake.

Fig. 2. Time-frequency representation (Spectrogram) of accelerograms recorded during the
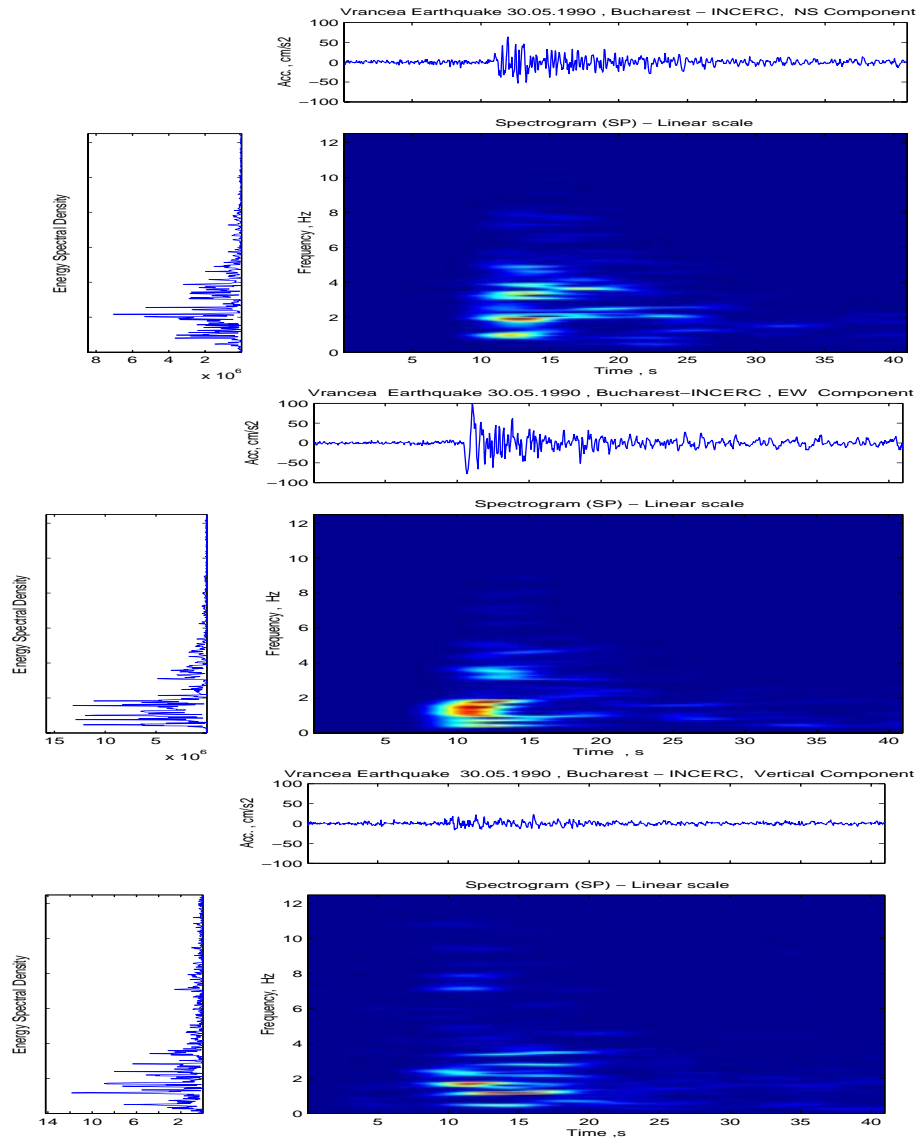1986 Vrancea earthquake.

Fig. 3. Time-frequency representation (Spectrogram) of accelerograms recorded during the
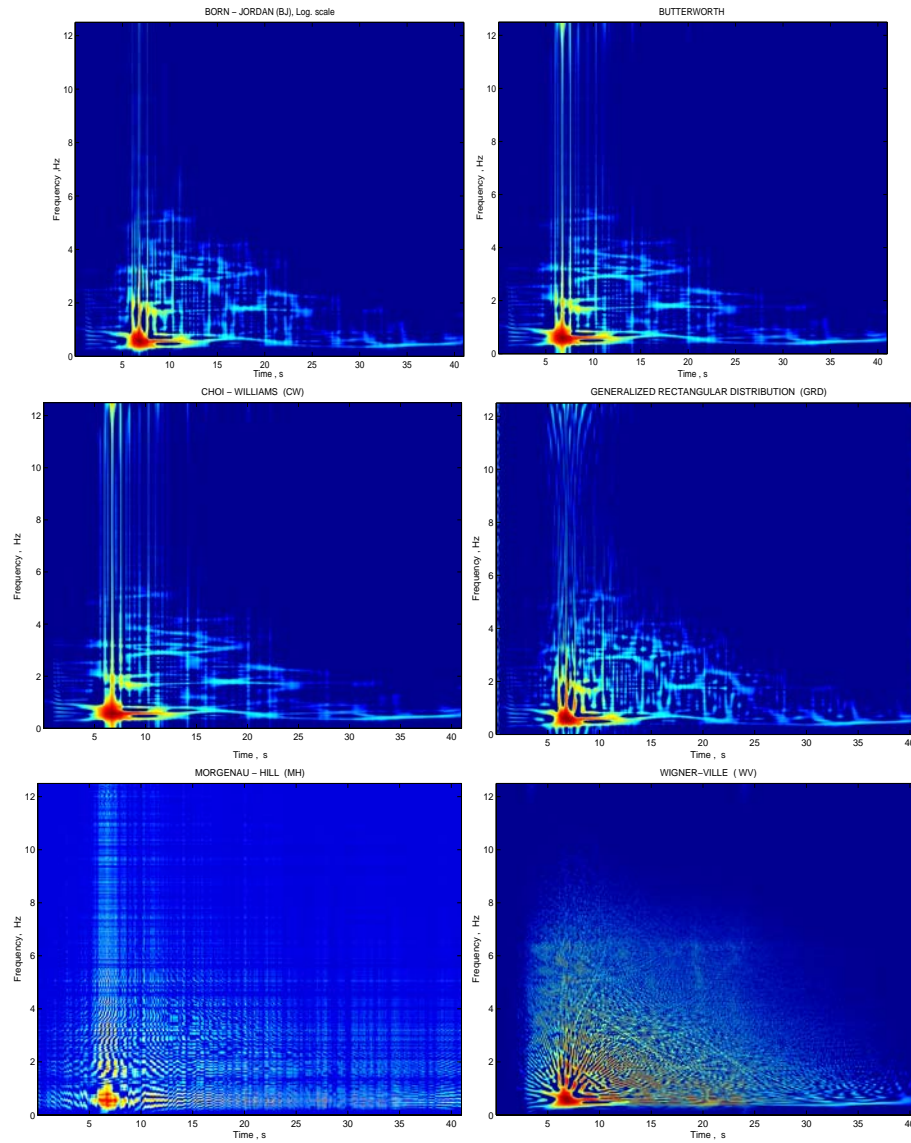1990 Vrancea earthquake.

Fig. 4. Different time-frequency distributions (log-scale spectral ordinates) of NS component of recorded accelerogram at Bucharest-INCERC during the 1977 Vrancea earthquake.
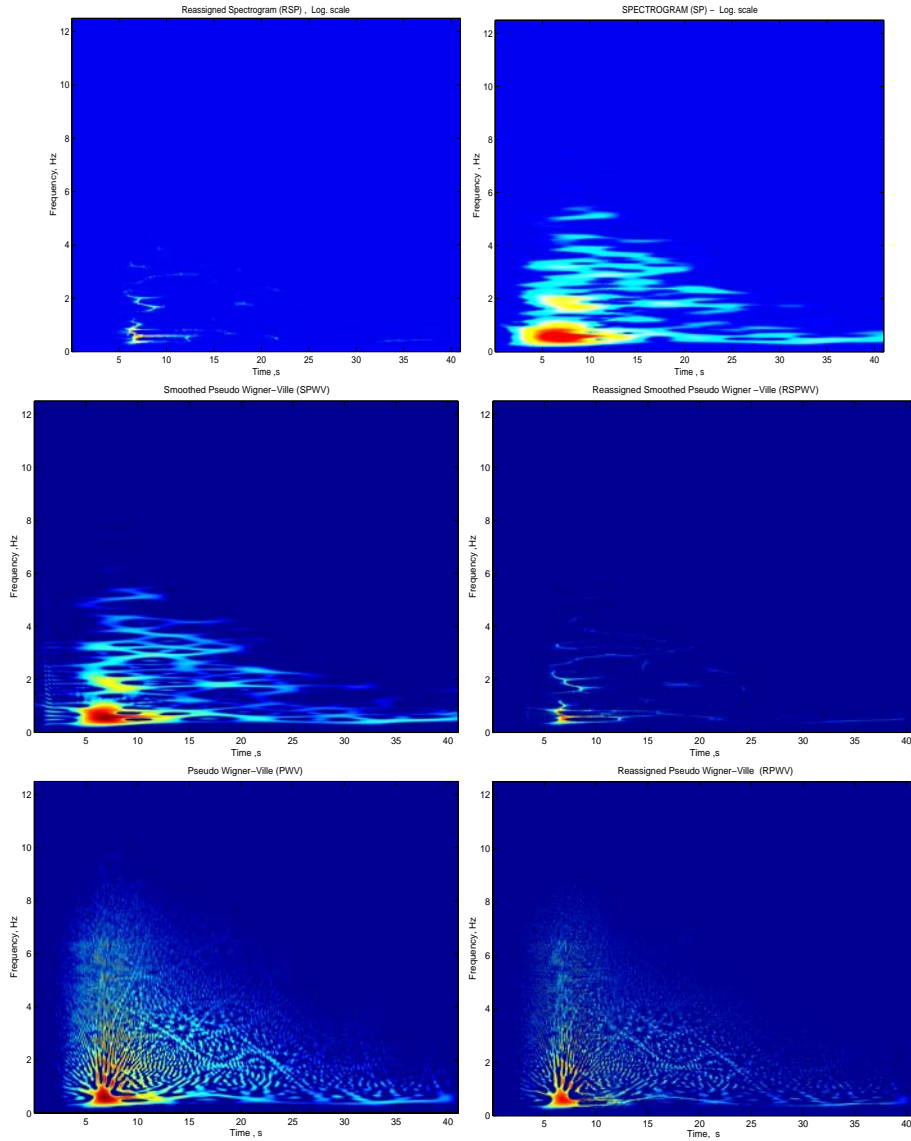
Fig. 5. Different time-frequency distributions (log-scale spectral ordinates) of NS component of recorded accelerogram at Bucharest-INCERC during the 1977 Vrancea earthquake.

Vrancea Earthquake 4.03.1977 , Bucharest – INCERC , NS Component

Vrancea Earthquake 4.03.1977, Bucharest – INCERC, EW Component

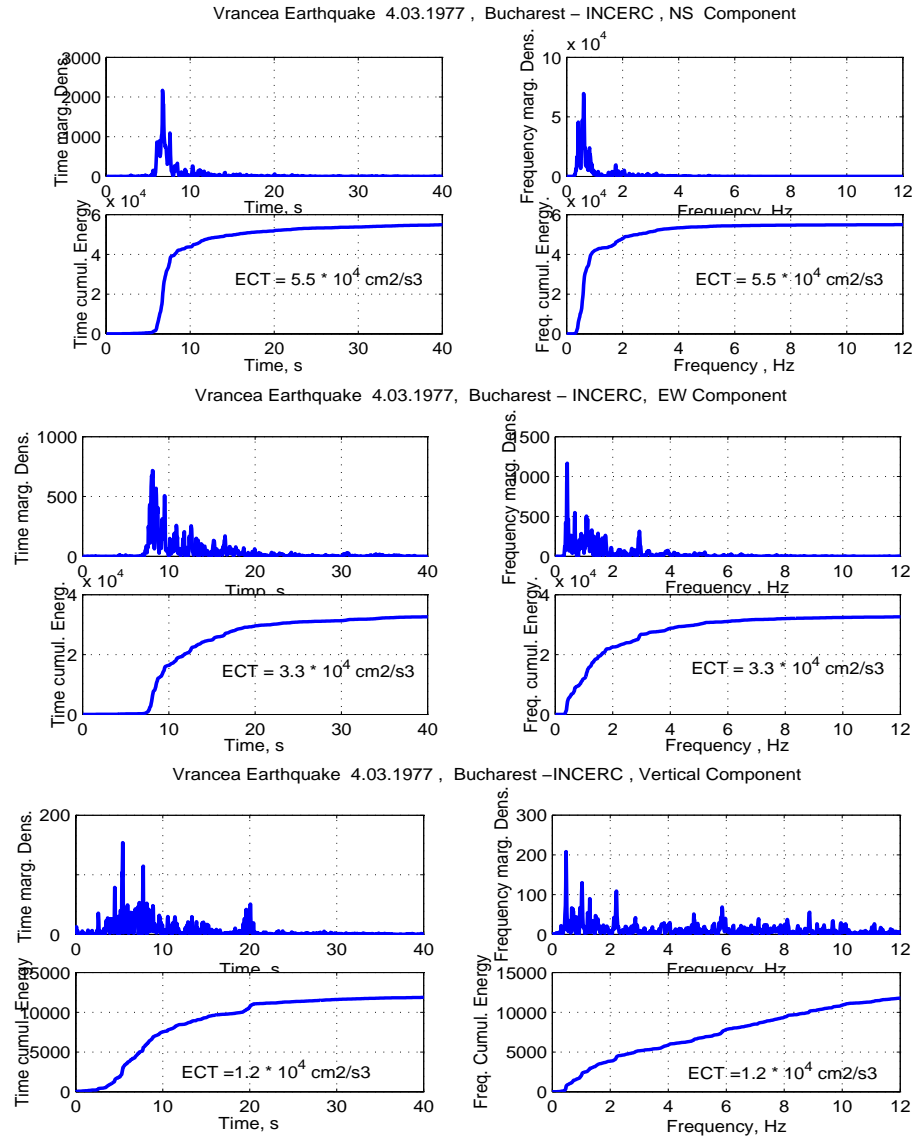Vrancea Earthquake 4.03.1977 , Bucharest –INCERC , Vertical Component

Fig. 6. Marginal densities and cumulative energy distributions of acceleration components recorded at Bucharest-INCERC during the 1977 Vrancea earthquake.